ChemistryOpen

Review
doi.org/10.1002/open.202200124

Chemistry Europe
European Chemical Societies Publishing

www.chemistryopen.org

In Vivo Imaging for the Visualization of Extracellular Vesicle-Based Tumor Therapy

Anqi Jiang, Weidong Nie, and Hai-Yan Xie*[a]

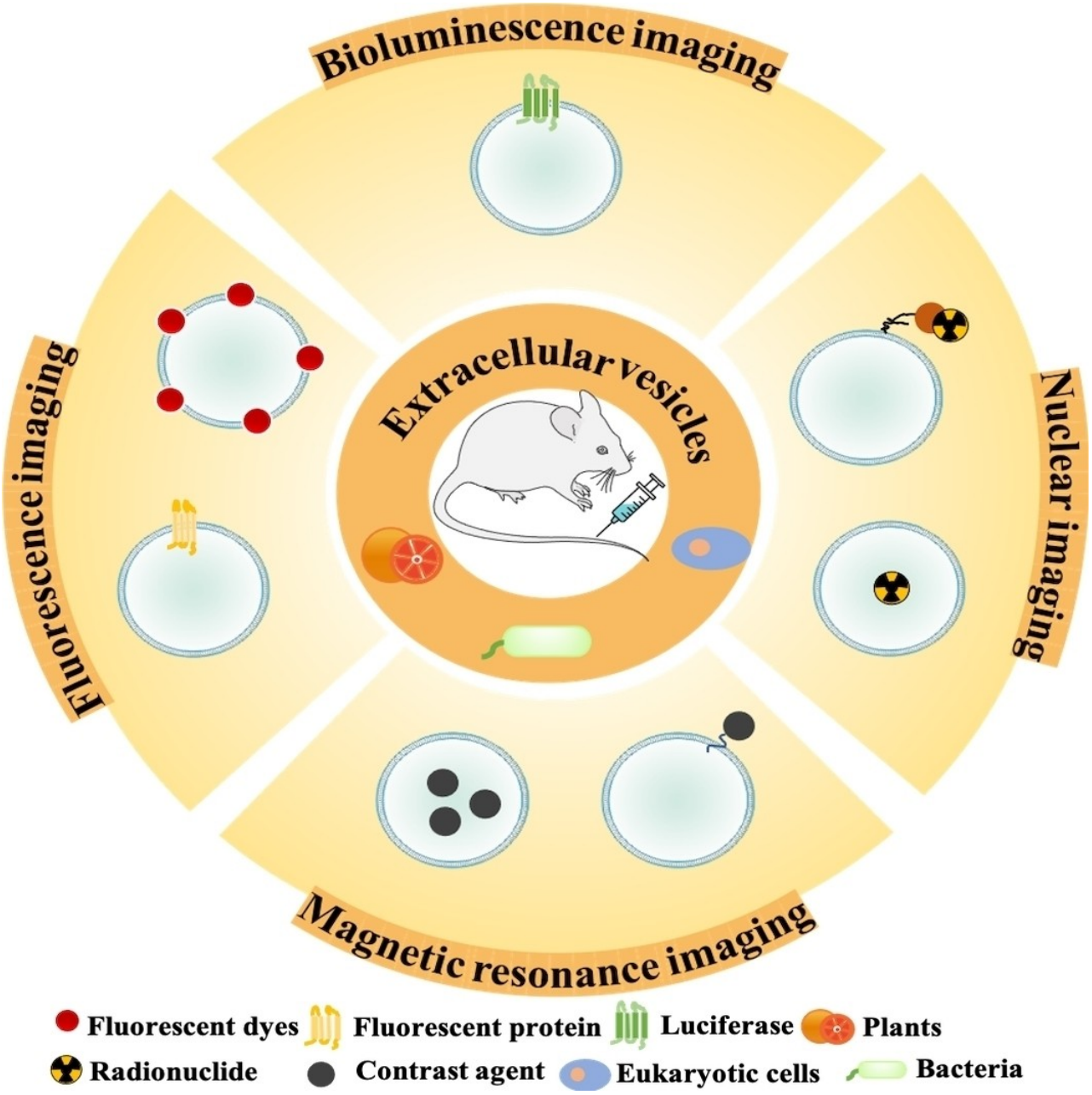

Extracellular vesicles (EVs) exhibiting versatile biological functions provide promising prospects as natural therapeutic agents and drug delivery vehicles. For future clinical translation, revealing the fate of EVs in vivo, especially their accumulation at lesion sites, is very important. The continuous development of in vivo imaging technology has made it possible to track the real-time distribution of EVs. This article reviews the applications of mammal-, plant-, and bacteria-derived EVs in tumor therapy, the labeling methods of EVs for in vivo imaging, the advantages and disadvantages of different imaging techniques, and possible improvements for future work.

1. Introduction

Extracellular vesicles (EVs) are nano-vesicles with a lipid bilayer structure secreted by cells.[1] According to their size and biogenesis process, EVs can be mainly divided into three main types: exosomes, microvesicles (MVs), and apoptotic bodies.[2]

Exosomes with a diameter about 40–100 nm are released as a consequence of multivesicular endosome fusion with the plasma membranes.[3] MVs originated from plasma membranes are about 100–1000 nm in diameter.[3] Apoptotic bodies have larger sizes from 500 nm to 5 μm, and are secreted by dying cells or apoptotic cells.[3] EVs carry a variety of parental cell-derived bioactive components, such as proteins, lipids, mRNA/miRNA, DNA and others, exhibiting good biocompatibility, lesion-targeting behavior, immunoregulation, and abilities to cross physiologic barriers.[4] These unique features and functions make them emerging candidates as therapeutic agents and drug delivery vehicles.

Monitoring the pharmacokinetics (half-life, biodistribution, clearance) of administrated EVs contributes to selecting suitable EVs derivation and formulating administration protocols so as to improve drug delivery efficiency.[5] Currently, two main engineering strategies have been developed to label EVs: direct labeling (direct interaction of EVs with lipophilic dyes, radionuclides, contrast agents, etc.) and indirect labeling (genetic engineering of parental cells with fluorescent reporter proteins or luciferase, and then collecting the released EVs; Figure 1). However, EVs are difficult to be tracked in living organisms because of their small size, rapid dispersion in body fluids, and similar composition to body cells.[6–7] Therefore, reliable engineering methods and highly sensitive imaging techniques are necessary for EVs visualization.

In this review, we firstly introduced different EVs that have been applied in tumor therapy. Then, we summarized the labeling methods of EVs for molecular imaging, the advantages and disadvantages of different imaging techniques, and the possibility of future clinical translation to enhance the understanding of the role of EVs in tumor therapy.

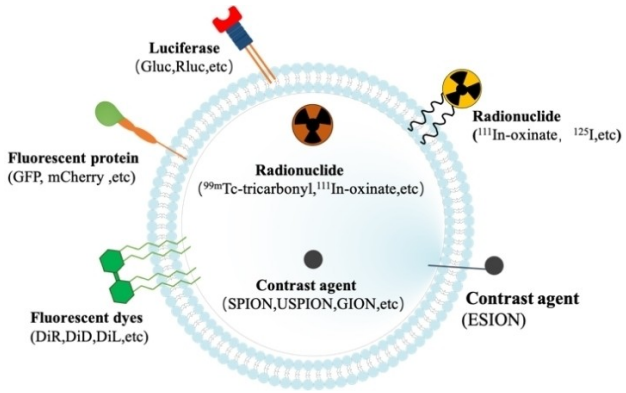

Figure 1. Various molecular imaging techniques to label extracellular vesicles for in vivo tracking. Lipophilic fluorescent dyes and genetically engineered fluorescent protein are used for fluorescence imaging; luciferase is used for bioluminescence imaging; radionuclide and contrast agents can be inserted into the membrane of EVs or loaded into the cavity of EVs for nuclear imaging or magnetic resonance imaging.

2. The Sources of EVs and their Application for Tumor Therapy

EVs can be obtained from a wide variety of sources and equipped with source-oriented functions. Here, we summarized the characteristics of EVs from different sources in tumor therapy (Table 1.).

2.1. Mammal Cell-Derived EVs

In mammals, EVs can be produced from almost any cells, such as immune cells and tumor cells.[8–9] It has been confirmed that immune cell-derived EVs are involved in intercellular communication, playing important roles in macrophage polarization, T cell and natural killer (NK) cell activation, as well as in antigen presentation. In the tumor microenvironment, almost all tumor cells and immune cells secrete EVs, correlating with the occurrence and development of tumors.[10] The biological functions of immune cell- and tumor cell-derived EVs will be discussed in further detail below.

[a] *A. Jiang, Prof. Dr. W. Nie, Prof. Dr. H.-Y. Xie*
School of Life Science
Beijing Institute of Technology
Beijing 100081 (P. R. China)
E-mail: hyanxie@bit.edu.cn

Part of a joint Special Collection of ChemistryOpen, Analysis & Sensing and *Chemistry–Methods* focusing on "Biosensing and Imaging: Methods and Applications". Please visit chemistryopen.org/collections to view all contributions.

Table 1. Characteristics and advantages of EVs from different sources.

Source	Type of cells	Advantages	Function	Ref.
Mammal	M1 macrophages	active targeting ability, good biocompatibility	pro-inflammatory, ability to repolarize M2 to M1, delivery vehicle	[13]
	Mature dendritic cells	good biocompatibility, tumors, lymph nodes target ability	regulate T cell, activate NK cell tumor vaccine, delivery vector	[24]
	Natural killer cells	immune stimulation, safety, strong killing ability	immune stimulation, delivery vehicle	[28]
	Tumor cells	homologous targeting ability	antigen, delivery vehicle	[35]
Plant	Plant roots, leaves, fruits, and seeds	wide range of sources, good biocompatibility, stable	regulate animal cell mRNA, delivery vehicle	[37-43]
Bacteria	Gram-negative bacteria	high yield, small particle size, easy genetic engineering,	immune adjuvant, delivery vehicle	[47]

2.1.1. Immune Cell-Derived EVs

The immune system contains multiple immune cells that play vital roles in maintaining the homeostasis of the internal environment. There are many intercellular communication pathways in the immune system, such as the release of factor signals, or direct contact between cells. In addition, the secretion of EVs from immune cells is also an important communication pathway.[11] Immune cell-derived EVs (IDEVs) are loaded with a variety of signaling molecules, such as proteins, lipids, DNA, and RNA.[12–14] When IDEVs are released, they can be endocytosed by recipient cells, thus completing the information transmission. Raposo et al. first demonstrated that immune cell-derived exosomes shared similar functions with their parental cells by verifying that B cell-derived exosomes possess MHC II complexes on the surface, which can induce T cell immune responses.[15] Significantly, the immune system can be effectively activated and then trigger the secretion of EVs to enhance the immune response upon the appearance of danger signals. In addition to being natural bioactive materials, IDEVs can be used as drug carriers for the delivery of nucleic acid or chemotherapeutic drugs.[16–17] IDEVs can effectively avoid the rapid clearance by the body's immune system, thus improving the drug delivery efficiency and reducing the side effects. Currently, three representative immune cell-derived EVs have been widely used in tumor therapy: M1 macrophage-derived EVs (M1EVs), dendritic cell-derived EVs (DCEVs), and NK cell-derived EVs (NKEVs).

Macrophages display noticeable plasticity and are generally defined as two phenotypes: M1- and M2- phenotypes. M1 macrophages have antitumor bioactivity, and they can produce pro-inflammatory cytokines, including interleukin-6 (IL-6), interleukin-12 (IL-12), and interferon-γ (IFN-γ).[18] In contrast, M2 macrophages can promote tumor growth and cause a negative effect on tumor therapy. M1 macrophage-derived EVs (M1EVs) carry a variety of chemokines and can home to the tumor sites, and then induce pro-inflammatory effects.[19] Moreover, M1EVs can polarize M2 macrophages into M1 phenotype, further improving the anti-tumor immunity and inhibiting tumor growth.[16]

DCEVs carry multiple functional molecules, such as antigen presentation molecules (MHCI and MHCII), co-stimulatory molecules (CD80, CD86), adhesion molecules (intercellular adhesion molecule 1 (ICAM-1), integrins), and NK modulation molecules (TNF-α, interleukin 15 receptor α (IL-15Rα), NKG2D-L).[20–25] DCEVs display different anti-tumor effects via multiple mechanisms. Firstly, mature DCEVs can directly present the exogenous peptide-loaded MHC (pMHC) to $CD4^+$ and $CD8^+$ T cells, thereby

Anqi Jiang is a master candidate of Beijing Institute of Technology. She received her B.Sc. in 2019 from the College of Life Science in Sichuan Normal University. Her research interests focus on the biomedical applications of bacterial outer membrane vesicles.

Weidong Nie is an associate professor of Beijing Institute of Technology. He received his Ph.D. in Chemical Engineering and Technology from Beijing Institute of Technology in 2020. His research interests focus on developing biomimetic nano-bioplatforms.

Hai-Yan Xie is a professor of Beijing Institute of Technology. She received her Ph.D. in Analytical Chemistry from Wuhan University in 2004. From 2013 to 2014, she worked as a visiting scholar at Stanford University. In 2020, she obtained the support of the National Science Fund for Distinguished Young Scholars in China. Her research focuses on bioimaging and nanobiomedicine.

inducing antigen-specific responses to suppress tumor growth.[26–27] Additionally, EVs derived from the antigen-loaded DC can be internalized by other DCs as a source of tumor antigen, which can also effectively stimulate the maturation of DCs, and then be presented to naïve, primed, or memory T cells.[28–29] Due to their versatility, DCEVs have been developed as novel tumor vaccines. Lu et al. investigated the efficiency of EVs from hepatocellular carcinoma (HCC) antigen-expressing DCs in three different HCC mouse models and proved the HCC treatment capability of DCEVs.[30] Significantly, DCEVs also promote the killing of tumors by activating NK cells.[31]

Studies have shown that NKEVs inherit many NK cell membrane molecules and contents, including the typical membrane marker CD56, the apoptosis-inducing FAS ligand (FASL), the activating receptor NK group 2D (NKG2D), and the cytotoxic molecules (perforin, granzymes et al.).[32–33] Many researchers proved the therapeutic efficacy of NKEVs against a variety of cancers, such as melanoma, leukemia, neuroblastoma, and glioblastoma.[34–37] Zhu et al. first demonstrated the anti-tumor effects of NKEVs in vivo. They injected activated-NKEVs into a melanoma mouse model in situ, and the tumor growth was significantly inhibited after treatment.[34] NKEVs can not only kill tumor cells through various mechanisms but also reprogram the immunosuppressive environment by activating other immune cells.[38]

2.1.2. Tumor Cell-Derived EVs

Recently, tumor cell-derived MVs have attracted much attention because of the inherited tropism for their parental cells.[39–40] Zuo et al. used tumor-cell released microvesicles to load drugs and achieved highly effective antitumor effects through the specific tumor-targeting ability of MVs.[41] Moreover, irradiated tumor-cell released MVs (RT-MVs) exhibit unique and broad antitumor abilities, and the yield of RT-MVs is significantly higher than that of unirradiated tumor cell-derived MVs. Wan found that, upon injection of RT-MVs into tumor-bearing mice, substantial amounts of RT-MVs were endocytosed by M2 tumor-associated macrophages (M2-TAMs), which were then polarized to anti-tumoral M1 macrophages.[42] RT-MVs expand the application of tumor-derived EVs and provide new candidates for antitumor therapy carriers. Furthermore, RT-MVs can be obtained from autologous dissected primary tumor cells, thus providing a potentially personalized cancer treatment solution. However, the prospect of tumor cell-derived EVs is uncertain in view of the potential risk of promoting tumor metastasis.

2.2. Plant Cell-Derived EVs

Plant-derived EVs (PDEVs) can also be used for tumor therapy and have attracted more and more interest. PDEVs can be obtained from different parts of plants, such as roots, stems, leaves, fruits, and seeds, and even from dried plant materials.[43–49] They contain abundant microRNAs (miRNAs) that are key regulators of gene expression. Xiao et al. investigated the types of miRNAs from 11 different fruits and vegetables, and 418 different miRNAs were identified. They found that highly expressed miRNAs are closely related to inflammatory response and cancer-related pathways, and in vitro experiments proved that miRNAs in PDEVs can modulate animal mRNAs.[43] Chin et al. found that miR159 enriched in *Arabidopsis*-derived EVs that could significantly inhibit the growth of xenograft breast tumors in mice.[44] Besides, the researchers found that ginseng-derived EVs can significantly promote the polarization of M2 macrophages to M1 macrophages and increase the content of reactive oxygen species at the tumor sites, thus significantly suppressing the growth of melanoma.[45]

Except for the antitumor functions, PDEVs can also be used as drug carriers. Garaeva et al. successfully used natural grapefruit-derived extracellular vesicles (GF-EVs) to effectively deliver exogenous proteins into both human peripheral blood mononuclear cells and colon cancer cells.[46] Another study showed that doxorubicin-loaded natural GF-EVs can bypass the blood-brain barrier and exert significant anti-glioma efficacy in vivo.[50] PDEVs have good biocompatibility and are nontoxic to human cells. In addition, they are highly stable under various environmental conditions, and can even resist the degradation by certain digestive enzymes, exhibiting great potential in tumor therapy.[51]

2.3. Bacterial-Derived EVs

The normal growth process of Gram-negative bacteria is usually accompanied by the shedding of extracellular outer membrane vesicles (OMVs). Compared with EVs derived from other sources, OMVs have a smaller size, thus stronger passive targeting ability to tumor sites. OMVs contain numerous components of their parental bacteria, especially, abundant lipopolysaccharide (LPS) molecules and outer membrane proteins on the surface of OMVs. These components are vital parts of the pathogen-associated molecular pattern (PAMP), which can be recognized and phagocytosed by antigen-presenting cells (APCs), thereby activating immune responses.[52] OMVs are often applied as drug carriers and immune adjuvants for tumor therapy. Guo et al. used OMVs to co-load chemotherapeutic drugs paclitaxel (PTX) and siRNA, and this composite nano OMVs system successfully regulated the tumor metabolic microenvironment and suppressed tumor growth.[53] Although effective, a high dose of OMVs can cause a strong immune storm, and thus serious side effects. Therefore, how to use OMVs for both effective and safe treatment is still a problem to be solved.

3. In Vivo Imaging of EVs

As therapeutic delivery vehicles, EVs play an important role in tumor diagnosis and treatment. To facilitate the clinical translation of EVs, it is essential to study the visualization of EVs in vivo. Various molecular imaging techniques such as fluorescence imaging (FLI), bioluminescence imaging (BLI),

Table 2. Comparison between different imaging modalities.

Imaging modality	Advantage	Disadvantage	Ref.
FLI	Medium sensitivity Low cost Easy operation	Limited tissue penetration Low spatiotemporal resolution	[56,57]
BLI	High sensitivity High signal-to-noise ratio	Complex operation Reaction substrate required Limited tissue penetration Low spatiotemporal resolution	[62–64]
PET or SPECT	High sensitivity High spatiotemporal resolution Highest tissue penetration	High cost Radiation	[70–72]
MRI	High resolution Good tissue contrasts	Lowest sensitivity High cost	[81–83]

nuclear imaging (PET/SPECT), and magnetic resonance imaging (MRI), have been applied to monitor the biodistribution of EVs in vivo. The labeling methods of EVs are mainly divided into direct and indirect labeling.[54–55] Direct labeling refers to the direct interaction of EVs with labeled molecules, such as lipophilic dyes, radionuclides, MRI contrast agents, and others. Indirect labeling requires genetic engineering of parental cells and collection of EVs released by these cells, such as fluorescent reporter proteins, luciferase used in BLI. FLI is the most commonly used imaging method to study the visualization of EVs at tumor sites. Near-infrared fluorescent dyes can label EVs by direct incubation and are inexpensive. However, near-infrared dyes are limited by the depth of tissue penetration. BLI is the imaging method with the highest sensitivity and high signal-to-noise ratio currently known. However, it requires indirect labeling of EVs through genetic engineering, requires injection of reaction substrates before imaging, and is limited by the depth of tissue penetration. Nuclear imaging and MRI are commonly used in clinical medical imaging. Nuclear imaging is also the most popular imaging modality at present, and the radioisotopes used to label EVs are not limited by the depth of tissue penetration. However, radioisotopes are expensive, dangerous, and need to be used by professional personnel. Compared with nuclear imaging, MRI imaging is safer and has higher tissue penetration and spatial and temporal resolution. However, its low sensitivity and high price also limit further applications (Table 2).

3.1. In Vivo Fluorescence Imaging of EVs

FLI is the most widely used imaging strategy to investigate the biodistribution of EVs in vivo because of the obvious advantages such as non-invasiveness, easy operation, and real-time monitoring. The fluorophores commonly used for EVs labeling include fluorescent proteins and lipophilic fluorescent dyes.

EVs have a phospholipid bilayer structure and are easily labeled by lipophilic dyes, such as PKH, dialkylcarbocyanines, cyanine dyes, and others. Furthermore, near-infrared dyes (NIRs) are suitable for non-invasive imaging of EVs in vivo due to the low autofluorescence of biological tissues in the 700–900 nm spectral range and the deep penetration of NIR light. The results of fluorescence imaging showed that different EVs display different targeting ability and specificity. Zhang et al. studied the tumor-targeting ability of DiR-labeled neutrophil-derived EVs and found that the fluorescent signal was mainly localized in the tumors after 72 h injection.[56] Lin et al. found that a large amount of iRGD-modified exosomes (iRGD-exo) could reach the tumor sites 6 h post-injection.[57] Gunassekaran et al. used IL4RPep-1 to modify the surface of M1EVs and labeled them with DiD dye.[16] Two hours after intravenous injection, IL4R-Exo was localized at the tumor sites with a four times higher fluorescence intensity than that of the control. BODIYPY is a NIR fluorescent dye that can specifically act on neutral lipids oil droplets, and can thus be used to label EVs. Guo et al. used BODIPY to label OMV-based paclitaxel (PTX) and the DNA damage response 1 (Redd1)-siRNA drug delivery system and found that the accumulation of siRNA@M-/PTX-CA-OMVs at the tumor sites was significantly enhanced 24 h post-injection.[53] Recently, Wang et al. reported that the accumulation of neutrophil-derived exosomes (NEs-Exo) in the C6-Luc glioma was clearly observed 24 h after intravenous injection and gradually increased with time. Their research results revealed that NEs-Exo can cross the blood-brain barrier (BBB), providing a new drug delivery option for the treatment of brain diseases[58] (Figure 2). Niu et al. found that Cy7 labeled grapefruit-derived EVs could also cross the blood-brain barrier/blood-(brain tumor) barrier.[50]

The way to label EVs with fluorescent proteins (FPs) is an indirect one. By using genetic engineering techniques, fluores-

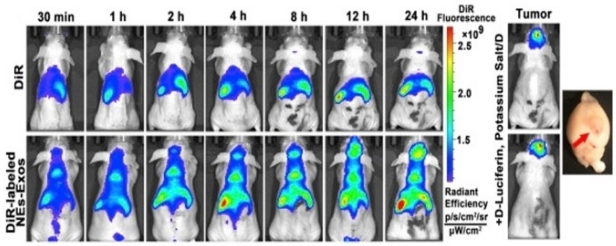

Figure 2. Fluorescence imaging of DiR and DiR-labeled NEs-Exos in brain tissue of C6-Luc glioma-bearing mice. Images were obtained at 30 min and 1, 2, 4, 8, 12, and 24 h post-injection. Adapted from Ref. [58] with permission. Copyright 2021, Elsevier.

cent protein reporter genes are fused to the specific genes of membrane proteins (e.g., CD9, CD63, CD81, etc.). The constructed plasmid is then transfected into target cells, and then the FP labeled EVs can be isolated. FP-labeling is specific, but the signal is usually not strong enough for in vivo imaging. Wiklander et al. obtained the EGFP-tagged EVs by transfecting the CD63-EGFP plasmid into HEK293T cells.[59] The results showed that only 20% of EVs were labeled with EGFP, and the fluorescence signal was hardly detectable 24 h post-injection. Lazaro-Ibanez et al. fused the mCherry fluorescent protein with a CD63 marker to label the Expi293F cell-derived EVs.[60] Nonetheless, in vivo FLI also failed to detect EVs in real time because of the high auto-fluorescence of mammalian tissues.

3.2. In Vivo Bioluminescence Imaging of EVs

Bioluminescence is generated by the chemical reaction between luciferase and a special substrate. Compared with fluorescence imaging, the generation of bioluminescence imaging (BLI) does not require external excitation, thus avoiding the interference of auto-luminescence of mammalian tissues. Therefore, bioluminescence imaging has an extremely high signal-to-noise ratio and is suitable for real-time tracking, and even for in vivo quantification.

Bioluminescence imaging of EVs requires the labeling of vesicles with a luciferase reporter protein. The luciferase genes (*Gaussia* luciferase [Gluc], *Renilla* luciferase [Rluc], and firefly luciferase [Fluc], etc.) are fused with different genes of membrane proteins (e.g., ALIX, TSG101, tetraspanins like CD9, CD63, CD81, etc.) on target cells to form an engineered vector plasmid.[61] Then, the plasmid is transfected into target cells, which can then be cultured for an appropriate time to then release EVs that carry the corresponding reporter proteins. Before imaging, a suitable substrate (RLuc/GLuc-Coelenterazine, FLuc-D-luciferin) is injected into the organism to visualize the biodistribution of EVs.

Takahashi et al. successfully fused *Gaussia* luciferase (Gluc) and truncated lactadherin, a membrane-associated protein mainly found in exosomes, and formed a fusion protein gLuc-lactadherin. Then, the fusion protein was transfected into B16-BL6 cells, with the labeled EVs obtained, which were then intravenously injected into mice. The results showed that EVs firstly appeared in the liver and then in the lungs. Furthermore, the pharmacokinetic analysis showed that the half-life of labeled EVs is very short, and they were rapidly cleared from the body soon after injection.[62] Imai et al. used the same labeling method to investigate the clearance mechanism of B16-BL6 cells-derived EVs.[63] They found that the clearance of B16-BL6 cells-derived EVs in macrophage-depleted mice was much slower than that in normal mice, indicating that macrophages played important roles in the clearance of intravenously injected EVs.

Lai et al. created a sensitive reporter (GLucB) for the labeling and multimodal imaging of HEK 293T-derived EVs by combining *Gaussia* luciferase and metabolic biotinylation.[64] The bioluminescence and fluorescence-mediated tomography imaging showed that obvious signals of EVs appeared in the spleens and livers 30 min post-injection, and a significant accumulation of signals at tumor sites appeared 1 h post-injection. Monitoring EV signals in organs, blood, and urine, they furthermore found that EVs first underwent a rapid distribution phase followed by a long elimination phase via the hepatic and renal pathways of 6 h. Both two phases were faster than previously reported results (24 h) of dye-labeled EVs.

To investigate whether tumor-derived EVs can preferentially target their parent cells, Gangadaran et al. used *Renilla* luciferase (RLuc) to label thyroid cancer cell-derived EVs (RLuc-CAL62-EVs) and monitored their homologous targeting ability. The bioluminescence imaging revealed that RLuc-CAL62-EVs targeted the homologous tumors in mice within 30 min after intravenous injection[65] (Figure 3).

Although specific and reliable, there are still some limitations to bioluminescence imaging. Firstly, the imaging performance is also affected by the penetration depth of bioluminescence. Secondly, the BLI labeling process is complicated, requiring the transfection of reporter gene plasmids into target cells, which may affect the characteristics of EVs. Besides, BLI requires additional administration of substrates for luciferase. Moreover, the half-life of the substrate is very short (s–min), thus multiple injections of substrates are usually necessary, which can be toxic to the animal.

3.3. In Vivo Nuclear Imaging of EVs

Nuclear imaging using gamma- or positron-emitting radionuclides as imaging probes is widely used for preclinical trafficking.[66] Single-photon emission computed tomography

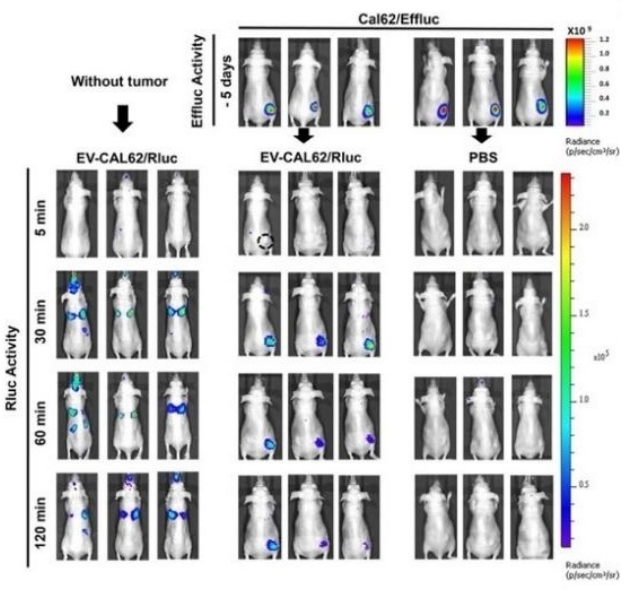

Figure 3. Bioluminescence imaging of CAL62/Rluc-labeled EVs in naïve or CAL62/Effluc tumor-bearing mice. Imaging was carried out at 5 min, 30 min, 60 min, and 120 min post-injection. Tumors are highlighted by black circles. Adapted from Ref. [65] with permission. Copyright 2021, Springer Nature.

(SPECT) and positron emission tomography (PET) are the main types of nuclear imaging. SPECT detects the gamma rays generated by the decay of radionuclides,[67] while PET detects a pair of photons in opposite directions with 511 keV energy produced by the decay of radionuclides.[68] Nuclear imaging has the advantages of high resolution, high sensitivity, deep tissue penetration, and three-dimensional quantification, so it has been clinically used for the diagnosis of tumors and brain diseases. Many radionuclides have already been approved for clinical use, so nuclear imaging is a good option to study the biodistribution of EVs in vivo.[69] Moreover, SPECT/PET is usually combined with CT to form a SPECT/CT or PET/CT system that has the characteristics of both functional and anatomical images.

^{99m}Tc is the most widely used radionuclide for in vivo imaging of EVs, mainly because of its low cost and good radiation properties. Varga et al. used ^{99m}Tc-tricarbonyl to label red blood cell, RBC-derived EVs by linking ^{99m}Tc-tricarbonyl with protein receptors on the EVs' surface. However, the radiolabeling yield was only determined to $38.8 \pm 6.2\%$ after incubation with RBC-derived EVs for 30 min.[70] Molavipordanjani et al. also used ^{99m}Tc-tricarbonyl to label HEK 293T-derived exosomes, and the labeling yield was determined to up to 96.5 %.[71] The biodistribution of EVs was studied in SKOV-3 tumor-bearing nude mice, and the results verified the satisfactory tumor-targeting accumulation ability of ^{99m}Tc-exosomes. María et al. used ^{99m}Tc to label milk-derived exosomes (MEXO) and studied their distribution in organisms.[72] In particular, the authors investigated the effect of administration routes on the in vivo distribution of MEXO. The results showed that the intravenously injected MEXO were mainly distributed in the liver and spleen, and mainly non-specific abdominal cavity distribution was found after intraperitoneal injection. In contrast, MEXO was mainly distributed in the gastrointestinal tract with a small amount of uptake in the brain after intranasal administration. The research on the different biodistribution of EVs is helpful for the determination of optimum administration routes on demand.

Although ^{99m}Tc is the most widely used radionuclide, its half-life is very short, which makes it unsuitable for long-term tracking. ^{111}In is another radionuclide that can be used for SPECT imaging. Its half-life can be as long as 2.8 days, so it is more suitable for long-term tracking of EVs in vivo. Smyth et al. used ^{111}In-oxinate to label exosomes derived from PC3 and MCF7 cells.[73] The results showed that the unmodified tumor-derived exosomes were rapidly cleared from the blood, less than 5 % of them were detained 3 h post-injection. This unmodified tumor-derived exosome had high uptake in the liver, spleen, and kidney, but low uptake at tumor sites at 24 h after injection. Faruqu et al.[74] used [^{111}In]DTPA to radiolabel the membrane surface of B16F10 cells-derived exosomes (Figure 4). The results of the study show that membrane labeling has higher radiolabeling efficiency and stability compared to intraluminal embedding. SPECT/CT imaging results showed that within 30 min of injection, free [^{111}In]DTPA complex had obvious signals in the kidney and bladder, indicating high excretion. In contrast, [^{111}In]DTPA-labeled B16F10 exosomes showed very high signal in liver and spleen within 30 min after injection and persisted until 24 h. However, neither signal was detected at the tumor site. The above studies demonstrate the limitation of unmodified tumor-derived exosomes in drug delivery. Exosomes derived from mesenchymal stem cells (MSCs) play an important role in immune regulation and tumorigenesis inhibition, so they are considered to be promising drug delivery vehicles for tumor therapy.[75–76]

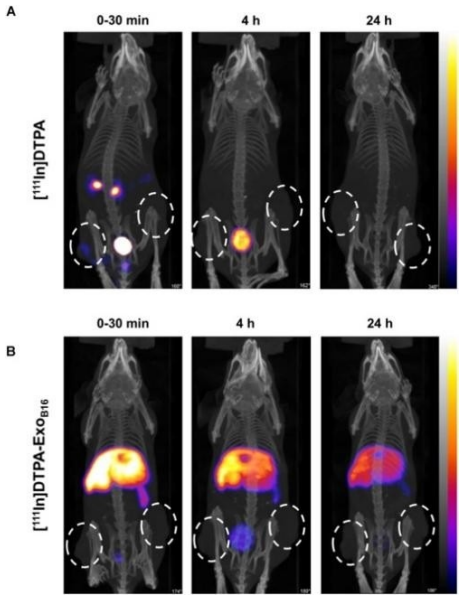

Figure 4. SPECT/CT imaging of free [^{111}In]DTPA complex and [^{111}In]DTPA-labeled B16F10 exosomes in melanoma-bearing mice. (A) Mice were injected intravenously with free [^{111}In]DTPA complex as control. (B) Mice were injected intravenously with [^{111}In]DTPA-labeled B16F10 exosomes. Imaging was conducted at 30 min, 4 h, and 24 h post-injection. Tumors are highlighted by white circles. Adapted from Ref. [74] with permission. Copyright 2019, Ivyspring International Publisher.

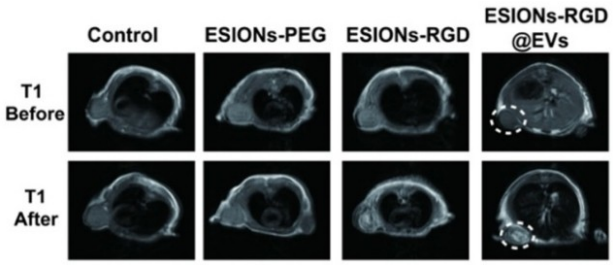

Figure 5. Magnetic resonance imaging of control, ESIONs-PEG, ESIONs-RGD and ESIONs-RGD@EVs in tumor-bearing mice. Imaging was conducted at 0 h and 2 h post-injection. Tumors are highlighted by white circles. Adapted from Ref. [89] with permission. Copyright 2021, Ivyspring International Publisher.

Cheng-Hsiu et al. used ^{111}In-oxinate to label MSCs-derived EVs (MSCs-EVs) and studied their behavior in vivo.[77] The image results showed that after intravenous injection, ^{111}In-MSC-EVs were mainly distributed in the liver, spleen, and kidney of normal mice.

Radioiodine (^{123}I, ^{124}I, ^{125}I, and ^{131}I) can also be used in EVs labeling.[78] ^{123}I and ^{131}I can be used for SPECT imaging, and ^{124}I

can be used for PET imaging. Morishita et al. transfected SAV-LA, a plasmid vector-encoding fusion protein, into B16BL6 cells and cultured them for EVs isolation. Then, EVs were incubated with (3-^{125}I-iodobenzoyl) norbiotinamide (^{125}I-IBB). Studies showed that ^{125}I-labeling of EVs via streptavidin-biotin interaction is a useful method for quantitative evaluation of EVs in vivo. However, genetic modification for radiolabeling is still a challenge in clinical translation. Moreover, protein variation on the surface of EVs may affect their interactions with recipient cells.[79]

3.4. In Vivo Magnetic Resonance Imaging of EVs

Magnetic resonance imaging (MRI) is a non-invasive imaging technique that can generate high-resolution anatomical images to identify structural abnormalities and lesions in the body. To enhance imaging contrast and improve diagnostic accuracy, contrast agents (CAs) are usually used.[80] CAs can change the relaxation times ($T_{1/2}$) of protons in local tissues and enhance the contrast with surrounding tissues. CAs can be principally divided into two basic types: T_1 contrast agents and T_2 contrast agents. T_1 contrast agents, such as Gd-DTPA and Mn-DPDP, are also called positive contrast agents, which can reduce the spin-lattice relaxation time T_1, thus strengthening the signal. T_2 contrast agents are known as negative contrast agents, reducing the spin-spin relaxation time T_2 and T_2* and resulting in reduced signal intensity.

Due to the non-invasive and high-resolution characteristics of MRI, researchers used MRI to study the biodistribution of EVs by loading CAs into EVs. T_2 magnetic agents such as superparamagnetic iron oxide nanoparticles (SPIONs) and ultrasmall superparamagnetic iron oxide nanoparticles (USPIONs) are widely used in clinical MRI. Hu et al. used melanoma exosomes to load SPIONs by electroporation, and then the SPIONs-loaded EVs were injected into the feet of mice and the MRI results showed that EVs preferentially migrate to draining lymph nodes 48 h after injection.[81] Compared with SPION, USPION has better magnetic properties and imaging effects. Busato et al. labeled adipose stem cells with USPIOs and then collected the excreted EVs.[82] The MRI results revealed that USPIO-loaded EVs were clearly detectable in the muscular tissues. Although this indirect labeling method can protect the integrity of EVs, the concentration of USPIONs loaded in EVs is lower (0.643 μg of iron per 100 μg of EV proteins). To track the distribution of EVs, it is necessary to inject a high dose of EVs, and excessive injection may induce adverse effects in the body.

As an alternative to electroporation, CAs can also be loaded into EVs by continuous extrusion. Since the cell membrane is fluid, the integrity of the membrane will not be destroyed after continuous extrusion, and a high loading dose can be achieved. Bose et al. constructed a theranostic nano-delivery system by encapsulating gold-iron oxide nanoparticles (GIONs) into 4T1-derived exosomes through continuous extrusion.[83] GIONs have both SPION properties for MRI and photothermal properties for photothermal therapy of tumors. The obtained TEV-GIONs were subsequently loaded with miRNA, forming a complex gene and photothermal therapy system. In vivo MRI results confirmed the specific accumulation of the system at tumor sites and its outstanding treatment performance.

Although great progress has been made, most available T_2 contrast agents face difficulties in clinical translation due to their intrinsic disadvantages, such as confusion with hypointense areas and blooming effects.[84] In contrast, T_1 contrast agents are more frequently used for accurate high-resolution imaging in clinics. As a typical T_1 contrast agent, gadolinium-based contrast agents (GBCAs) are widely used.[85] Rayamajhi et al. constructed Gd-labeled hybrid extracellular vesicles (Gd-HEV) by continuous extrusion.[86] Twenty-four hours after the tail vein injection, the contrast of Gd-HEV in the tumor areas was significantly enhanced compared with the control group (Magnevist®). However, the contrast enhancement effect was not impressive compared to the surrounding tissue. Quantitative determination by ICP-MS showed that only 0.63% of the injected dose per gram of tissue was localized in tumors. Such a low dose of localization may not be enough to provide a significant contrast enhancement. So, it is necessary to improve the initial injection dose to achieve a more obvious imaging effect. Yet, the use of high doses may cause systemic toxicity.[87] Therefore, it is necessary to develop safer contrast agents for EV labeling and in vivo imaging. A recent study evaluated the toxic effects and the subsequent tissue damage of three T_1 contrast agents: the clinically used GBCAs, the extremely small-sized iron oxide nanoparticles (ESIONs), and MnO NPs.[88] Compared with MnO NPs and GBCAs, ESIONs exhibited fewer side effects. Wu et al. linked ESIONs and glucose oxidase to the surface of hepatocellular carcinoma-derived EVs to form composite nanoparticles (GE@EVs) for tumor therapy and MRI imaging[89] (Figure 5) .GE@EVs significantly enhanced the T_1 signal in tumors 2 h after injection via the tail vein. Furthermore, residual ESIONs in tumor tissues could serve as contrast agents to real-time monitor HCC progression through MRI.

MRI is a promising method to track the distribution of EVs in vivo. However, some improvements are still needed to be made. Especially, although the resolution of MRI is high, its sensitivity is relatively low for tumor imaging. To overcome this limitation, it is necessary to develop new CAs, meanwhile improve their loading efficiency in EVs. On the other hand, the special microenvironment may be also used to improve the contrast between tumors and surrounding tissues.

4. Summary and Outlook

EVs possess versatile anti-tumoral effects. Immune cell-derived EVs in particular can regulate the tumor microenvironment and enhance antitumor effects. There are many types of plant-derived

EVs that can regulate the mRNA of tumor cells. Bacterial-derived EVs are powerful immune adjuvants that can be used to construct vaccines and initiate the anti-tumoral immune response. Meanwhile, EVs can be used as novel carriers for drug delivery.

Table 3. Strategies for in vivo tracking of EVs.

Modalities	Labeling molecule	Insertion site	Loading method	EV source	Animal model	Admin. route [a]	Tracking Time	Purpose	Ref.
FLI	EGFP	Membrane	Indirect (parent cell transfection)	HEK293T	C57BL/6 mice	IV	24 h	Biodistribution	[59]
	mCherry	Membrane	Indirect (parent cell transfection)	Expi293F cells	CT26 tumor-bearing mice	IV	24 h	Tumor Targeting	[60]
	DiR	Membrane	Direct incubation	neutrophil	HGC27 tumor-bearing mice	IV	12, 24, 48, 72 h	Tumor Targeting	[56]
	DiR	Membrane	Direct incubation	HEK293T	HCT116lohp tumor-bearing nude mouse	IV	0, 6, 24 h	Tumor Targeting	[57]
	DiR	Membrane	Direct incubation	neutrophil	C6-Luc glioma-bearing mice models	IV	0.5, 1, 2, 4, 8, 12, 24 h	Tumor Targeting	[58]
	DiD	Membrane	Direct incubation	macrophage	4T1 mouse breast tumor	IV	2 h	Tumor Targeting	[16]
	Cy7	Membrane	Direct incubation	grapefruit	glioma-bearing nude mice	IV	0.5, 3, 6, 12, 24, 48, 72, 96 h	Tumor Targeting	[50]
	Bodipy	Membrane	Direct incubation	E.coli BL21	triple-negative breast cancer model	IV	1, 2, 4, 8, 10, 12 h	Tumor Targeting	[53]
BIL	GLuc-lactadherin	Membrane	Indirect (parent cell transfection)	B16-BL6 murine melanoma cells	BALB/c mice	IV	10, 30, 60, 240 min	Biodistribution	[62]
	GLuc-lactadherin	Membrane	Indirect (parent cell transfection)	B16-BL6 murine melanoma cells	BALB/c mice(macrophage-depleted mice)	IV	10, 30, 60, 240 min	Biodistribution	[63]
	GLuc-biotinylation	Membrane	Indirect (parent cell transfection)	HEK293T	Gli36 human glioma-bearing mouse, nude mice	IV	30, 60 min	Biodistribution; Tumor Targeting	[64]
	Rluc	Intraluminal	Indirect (parent cell transfection)	Anaplastic thyroid cancer (CAL62) cell	naïve or CAL62/Effluc tumor-bearing mice	IV	5, 30, 60, 120 min	Tumor Targeting	[65]
	Fluc	Intraluminal	Indirect (parent cell transfection)	mesenchymal stem cells (MSCs)	breast cancer xenografts-bearing mice	IV	1, 24 h	Tumor Targeting	[61]
NI	^{99m}*Tc*-tricarbonyl	Membrane	Direct	red blood cell	BALB/c mice	IV	1 h	Biodistribution	[70]
	^{99m}*Tc*-tricarbonyl	Membrane	Direct	HEK 293T	SKOV-3-tumor-bearing nude mice	IV	4 h	Tumor Targeting	[71]
	^{99m}*Tc*	Membrane	Direct	milk	Balb/C mice	IV/IP/IN	5, 30, 60 min; 24 h	Biodistribution	[72]
	^{111}In-oxinate	Intraluminal	Direct	PC3/4T1/MCF7	4T1/PC3 tumor-bearing mice	IV/IT	30 min	Biodistribution Tumor Targeting	[73]
	^{111}In-oxinate	Intraluminal	Direct	mesenchymal stem cell	C57BL/6 mice	IV	1, 3, 6, 24 h	Biodistribution	[77]
	^{111}In-DTPA	Membrane	Direct	B16-BL6 murine melanoma	melanoma-bearing C57Bl/6 mice	IV	30 min; 4, 24 h	Tumor Targeting Biodistribution	[74]
	^{125}I	Membrane	Direct	B16-BL6 murine melanoma cells	BALB/c mice	IV	1, 30, 240 min	Biodistribution	[79]
MRI	SPION	Intraluminal	Direct electroporation	melanoma cell	C57BL/6 mouse model	ID	1, 48 h	Nodal trafficking	[81]
	USPION	Intraluminal	Indirect parent cell incubation	adipose stem cells	C57BL/6 mouse model	IM	1 h	Retention at injection site	[82]
	GION	Intraluminal	Direct extrusion	breast cancer cells	4T1 tumor-bearing mouse model	IV	12 d	Tumor Targeting	[83]
	GBCA	Intraluminal	Direct extrusion	mouse macrophage	osteosarcoma tumor-bearing mouse model	IV	24 h	Tumor Targeting	[86]
	ESION	Membrane	Direct incubation	hepatocellular carcinoma	HCC tumor-bearing mouse model	IV	2 h	Tumor Targeting	[89]

[a]: Abbreviations: IV, intravenous;IP, intraperitoneal; IN, intranasal; IT, intratumor; ID, intradermal; IM, intramuscular.

To promote EV-based drug delivery and tumor therapy, it is necessary to reveal the biodistribution of EVs in vivo, especially their accumulation at tumor sites, and different molecular imaging methods have been developed for this purpose as shown as an overview in Table 3. In this article, we summarized fluorescence imaging, bioluminescence imaging, nuclear imaging, and magnetic resonance imaging for monitoring the biodistribution of EVs in vivo. The fluorescence imaging labeling method is simple and the most used in observing EVs in vivo. However, its practical application is limited by the penetration depth. Bioluminescence imaging is highly sensitive, but labeling EVs through genetic engineering techniques might change the native characteristics of EVs. Nuclear imaging and MRI have already been commonly used in clinics, and they are also the most promising methods to visualize EVs in clinical. However, the risk of radioactive elements of nuclear imaging and the low sensitivity of MRI are needed to be addressed. In order to more accurately study the biodistribution of EVs in vivo, the combined use of multiple imaging methods, and the development of new labeling molecules and methods are worth being studied in the future.

Acknowledgements

This work was funded by the National Natural Science Foundation of China (21874011, 32101140), the National Science Fund for Distinguished Young Scholars (22025401), and the Beijing Institute of Technology Research Fund Program for Young Scholars. The authors thank Biological & Medical Engineering Core Facilities (Beijing Institute of Technology).

Conflict of Interest

The authors declare no conflict of interest.

Data Availability Statement

The data that support the findings of this study are available from the corresponding author upon reasonable request.

[1] R. Kalluri, V. S. LeBleu, *Science* **2020**, *367*, eaau6977.
[2] N. P. Hessvik, A. Llorente, *Cell. Mol. Life Sci.* **2018**, *75*, 193–208.
[3] L. Cabeza, G. Perazzoli, M. Peña, A. Cepero, C. Luque, C. Melguizo, J. Prados, *J. Controlled Release* **2020**, *327*, 296–315.
[4] S. Mathivanan, C. J. Fahner, G. E. Reid, R. J. Simpson, *Nucleic Acids Res.* **2012**, *40*, D1241–1244.
[5] F. J. Verweij, L. Balaj, C. M. Boulanger, D. R. F. Carter, E. B. Compeer, G. D'Angelo, S. El Andaloussi, J. G. Goetz, J. C. Gross, V. Hyenne, E. M. Krämer-Albers, C. P. Lai, X. Loyer, A. Marki, S. Momma, E. N. M. Nolte-'t Hoen, D. M. Pegtel, H. Peinado, G. Raposo, K. Rilla, H. Tahara, C. Théry, M. E. van Royen, R. E. Vandenbroucke, A. M. Wehman, K. Witwer, Z. Wu, R. Wubbolts, G. van Niel, *Nat. Methods* **2021**, *18*, 1013–1026.
[6] T. Lorenc, J. Chrzanowski, W. Olejarz, *Cancers (Basel).* **2020**, *12*, 3386.
[7] T. Yamashita, Y. Takahashi, Y. Takakura, *Biol. Pharm. Bull.* **2018**, *41*, 835–842.
[8] R. E. Veerman, G. Güçlüler Akpinar, M. Eldh, S. Gabrielsson, *Trends Mol. Med.* **2019**, *25*, 382–394.
[9] X. Tian, H. Shen, Z. Li, T. Wang, S. Wang, *J. Hematol. Oncol.* **2019**, *12*, 84.
[10] R. Xu, A. Rai, M. Chen, W. Suwakulsiri, D. W. Greening, R. J. Simpson, *Nat. Rev. Clin. Oncol.* **2018**, *15*, 617–638.
[11] C. Wen, R. C. Seeger, M. Fabbri, L. Wang, A. S. Wayne, A. Y. Jong, *J. Extracell. Vesicles* **2017**, *6*, 1400370.
[12] M. Record, K. Carayon, M. Poirot, S. Silvente-Poirot, *Biochim. Biophys. Acta* **2014**, *1841*, 108–120.
[13] B. K. Thakur, H. Zhang, A. Becker, I. Matei, Y. Huang, B. Costa-Silva, Y. Zheng, A. Hoshino, H. Brazier, J. Xiang, C. Williams, R. Rodriguez-Barrueco, J. M. Silva, W. Zhang, S. Hearn, O. Elemento, N. Paknejad, K. Manova-Todorova, K. Welte, J. Bromberg, H. Peinado, D. Lyden, *Cell Res.* **2014**, *24*, 766–769.
[14] H. Valadi, K. Ekström, A. Bossios, M. Sjöstrand, J. J. Lee, J. O. Lötvall, *Nat. Cell Biol.* **2007**, *9*, 654–659.
[15] G. Raposo, H. W. Nijman, W. Stoorvogel, R. Liejendekker, C. V. Harding, C. J. Melief, H. J. Geuze, *J. Exp. Med.* **1996**, *183*, 1161–1172.
[16] G. R. Gunassekaran, S. M. Poongkavithai Vadevoo, M. C. Baek, B. Lee, *Biomaterials* **2021**, *278*, 121137.
[17] M. S. Kim, M. J. Haney, Y. Zhao, V. Mahajan, I. Deygen, N. L. Klyachko, E. Inskoe, A. Piroyan, M. Sokolsky, O. Okolie, S. D. Hingtgen, A. V. Kabanov, E. V. Batrakova, *Nanomedicine* **2016**, *12*, 655–664.
[18] S. Gordon, P. R. Taylor, *Nat. Rev. Immunol.* **2005**, *5*, 953–964.
[19] P. Dalvi, B. Sun, N. Tang, L. Pulliam, *Sci. Rep.* **2017**, *7*, 9954.
[20] C. Admyre, S. M. Johansson, S. Paulie, S. Gabrielsson, *Eur. J. Immunol.* **2006**, *36*, 1772–1781.
[21] C. Théry, M. Boussac, P. Véron, P. Ricciardi-Castagnoli, G. Raposo, J. Garin, S. Amigorena, *J. Immunol.* **2001**, *166*, 7309–7318.
[22] S. I. Buschow, E. N. Nolte-'t Hoen, G. van Niel, M. S. Pols, T. ten Broeke, M. Lauwen, F. Ossendorp, C. J. Melief, G. Raposo, R. Wubbolts, M. H. Wauben, W. Stoorvogel, *Traffic.* **2009**, *10*, 1528–1542.
[23] E. Segura, C. Nicco, B. Lombard, P. Véron, G. Raposo, F. Batteux, S. Amigorena, C. Théry, *Blood* **2005**, *106*, 216–223.
[24] K. S. Reiners, J. Dassler, C. Coch, E. Pogge von Strandmann, *Front. Immunol.* **2014**, *5*, 91.
[25] S. Viaud, M. Terme, C. Flament, J. Taieb, F. André, S. Novault, B. Escudier, C. Robert, S. Caillat-Zucman, T. Tursz, L. Zitvogel, N. Chaput, *PLoS One* **2009**, *4*, e4942.
[26] M. F. S. Lindenbergh, W. Stoorvogel, *Annu. Rev. Immunol.* **2018**, *36*, 435–459.
[27] L. Zitvogel, A. Regnault, A. Lozier, J. Wolfers, C. Flament, D. Tenza, P. Ricciardi-Castagnoli, G. Raposo, S. Amigorena, *Nat. Med.* **1998**, *4*, 594–600.
[28] E. Segura, S. Amigorena, C. Théry, *Blood Cells Mol. Dis.* **2005**, *35*, 89–93.
[29] F. André, N. Chaput, N. E. Schartz, C. Flament, N. Aubert, J. Bernard, F. Lemonnier, G. Raposo, B. Escudier, D. H. Hsu, T. Tursz, S. Amigorena, E. Angevin, L. Zitvogel, *J. Immunol.* **2004**, *172*, 2126–2136.
[30] Z. Lu, B. Zuo, R. Jing, X. Gao, Q. Rao, Z. Liu, H. Qi, H. Guo, H. Yin, *J. Hepatol.* **2017**, *67*, 739–748.
[31] S. Munich, A. Sobo-Vujanovic, W. J. Buchser, D. Beer-Stolz, N. L. Vujanovic, *Oncoimmunology* **2012**, *1*, 1074–1083.
[32] L. Lugini, S. Cecchetti, V. Huber, F. Luciani, G. Macchia, F. Spadaro, L. Paris, L. Abalsamo, M. Colone, A. Molinari, F. Podo, L. Rivoltini, C. Ramoni, S. Fais, *J. Immunol.* **2012**, *189*, 2833–2842.
[33] A. Y. Jong, C. H. Wu, J. Li, J. Sun, M. Fabbri, A. S. Wayne, R. C. Seeger, *J. Extracell. Vesicles* **2017**, *6*, 1294368.
[34] L. Zhu, S. Kalimuthu, P. Gangadaran, J. M. Oh, H. W. Lee, S. H. Baek, S. Y. Jeong, S. W. Lee, J. Lee, B. C. Ahn, *Theranostics* **2017**, *7*, 2732–2745.
[35] C. S. Hong, P. Sharma, S. S. Yerneni, P. Simms, E. K. Jackson, T. L. Whiteside, M. Boyiadzis, *Sci. Rep.* **2017**, *7*, 14684.
[36] A. Shoae-Hassani, A. A. Hamidieh, M. Behfar, R. Mohseni, S. A. Mortazavi-Tabatabaei, S. Asgharzadeh, *J. Immunother.* **2017**, *40*, 265–276.
[37] L. Zhu, J. M. Oh, P. Gangadaran, S. Kalimuthu, S. H. Baek, S. Y. Jeong, S. W. Lee, J. Lee, B. C. Ahn, *Front. Immunol.* **2018**, *9*, 824.
[38] S. Fais, *Oncoimmunology* **2013**, *2*, e22337.
[39] L. T. Brinton, H. S. Sloane, M. Kester, K. A. Kelly, *Cell. Mol. Life Sci.* **2015**, *72*, 659–671.
[40] R. J. Lobb, L. G. Lima, A. Möller, *Semin. Cell Dev. Biol.* **2017**, *67*, 3–10.
[41] L. Zuo, W. Nie, S. Yu, W. Zhuang, G. Wu, H. Liu, L. Huang, D. Shi, X. Sui, Y. Li, H. Y. Xie, *Angew. Chem. Int. Ed.* **2021**, *60*, 25365–25371.
[42] W. Olejarz, A. Dominiak, A. Żołnierzak, G. Kubiak-Tomaszewska, T. Lorenc, *J. Immunol. Res.* **2020**, *2020*, 6272498.
[43] J. Xiao, S. Feng, X. Wang, K. Long, Y. Luo, Y. Wang, J. Ma, Q. Tang, L. Jin, X. Li, M. Li, *PeerJ* **2018**, *6*, e5186.
[44] A. R. Chin, M. Y. Fong, G. Somlo, J. Wu, P. Swiderski, X. Wu, S. E. Wang, *Cell Res.* **2016**, *26*, 217–228.

[45] M. Cao, H. Yan, X. Han, L. Weng, Q. Wei, X. Sun, W. Lu, Q. Wei, J. Ye, X. Cai, C. Hu, X. Yin, P. Cao, *J. Immunother. Cancer* **2019**, *7*, 326.
[46] L. Garaeva, R. Kamyshinsky, Y. Kil, E. Varfolomeeva, N. Verlov, E. Komarova, Y. Garmay, S. Landa, V. Burdakov, A. Myasnikov, I. A. Vinnikov, B. Margulis, I. Guzhova, A. Kagansky, A. L. Konevega, T. Shtam, *Sci. Rep.* **2021**, *11*, 6489.
[47] Y. Teng, F. Xu, X. Zhang, J. Mu, M. Sayed, X. Hu, C. Lei, M. Sriwastva, A. Kumar, K. Sundaram, L. Zhang, J. W. Park, S. Y. Chen, S. Zhang, J. Yan, M. L. Merchant, X. Zhang, C. J. McClain, J. K. Wolfe, R. S. Adcock, D. Chung, K. E. Palmer, H. G. Zhang, *Mol. Ther.* **2021**, *29*, 2424–2440.
[48] M. Regente, G. Corti-Monzón, A. M. Maldonado, M. Pinedo, J. Jorrín, L. de la Canal, *FEBS Lett.* **2009**, *583*, 3363–3366.
[49] E. Woith, M. F. Melzig, *Int. J. Mol. Sci.* **2019**, 20,357.
[50] W. Niu, Q. Xiao, X. Wang, J. Zhu, J. Li, X. Liang, Y. Peng, C. Wu, R. Lu, Y. Pan, J. Luo, X. Zhong, H. He, Z. Rong, J. B. Fan, Y. Wang, *Nano Lett.* **2021**, *21*, 1484–1492.
[51] P. Akuma, O. D. Okagu, C. C. Udenigwe, *Front. Sustain. Food Syst.* **2019**, *3*, 23.
[52] M. E. Kuipers, C. H. Hokke, H. H. Smits, E. N. M. Nolte-'t Hoen, *Front. Microbiol.* **2018**, *9*, 2182.
[53] Q. Guo, X. Li, W. Zhou, Y. Chu, Q. Chen, Y. Zhang, C. Li, H. Chen, P. Liu, Z. Zhao, Y. Wang, Z. Zhou, Y. Luo, C. Li, H. You, H. Song, B. Su, T. Zhang, T. Sun, C. Jiang, *ACS Nano* **2021**,*15*,13826–13838.
[54] Y. J. Li, J. Y. Wu, J. M. Wang, X. B. Hu, D. X. Xiang, *J. Controlled Release* **2020**, *328*, 141–159.
[55] S. Salunkhe, Dheeraj, M. Basak, D. Chitkara, A. Mittal, *J. Controlled Release* **2020**, *326*, 599–614.
[56] J. Zhang, C. Ji, H. Zhang, H. Shi, F. Mao, H. Qian, W. Xu, D. Wang, J. Pan, X. Fang, H. A. Santos, X. Zhang, *Sci. Adv.* **2022**, *8*, eabj8207.
[57] D. Lin, H. Zhang, R. Liu, T. Deng, T. Ning, M. Bai, Y. Yang, K. Zhu, J. Wang, J. Duan, S. Ge, B. Sun, G. Ying, Y. Ba, *Mol. Oncol.* **2021**, *15*, 3430–3446.
[58] J. Wang, W. Tang, M. Yang, Y. Yin, H. Li, F. Hu, L. Tang, X. Ma, Y. Zhang, Y. Wang, *Biomaterials* **2021**, *273*, 120784.
[59] O. P. Wiklander, J. Z. Nordin, A. O'Loughlin, Y. Gustafsson, G. Corso, I. Mäger, P. Vader, Y. Lee, H. Sork, Y. Seow, N. Heldring, L. Alvarez-Erviti, C. I. Smith, K. Le Blanc, P. Macchiarini, P. Jungebluth, M. J. Wood, S. E. Andaloussi, *J. Extracell. Vesicles* **2015**, *4*, 26316.
[60] E. Lázaro-Ibáñez, F. N. Faruqu, A. F. Saleh, A. M. Silva, J. Tzu-Wen Wang, J. Rak, K. T. Al-Jamal, N. Dekker, *ACS Nano* **2021**, *15*, 3212–3227.
[61] S. Kalimuthu, J. M. Oh, P. Gangadaran, L. Zhu, H. Won Lee, R. L. Rajendran, S. H. Baek, Y. H. Jeon, S. Y. Jeong, S. W. Lee, J. Lee, B. C. Ahn, *Stem Cells Int.* **2020**, *2020*, 8275897.
[62] Y. Takahashi, M. Nishikawa, H. Shinotsuka, Y. Matsui, S. Ohara, T. Imai, Y. Takakura, *J. Biotechnol.* **2013**, *165*, 77–84.
[63] T. Imai, Y. Takahashi, M. Nishikawa, K. Kato, M. Morishita, T. Yamashita, A. Matsumoto, C. Charoenviriyakul, Y. Takakura, *J. Extracell. Vesicles* **2015**, *4*, 26238.
[64] C. P. Lai, O. Mardini, M. Ericsson, S. Prabhakar, C. Maguire, J. W. Chen, B. A. Tannous, X. O. Breakefield, *ACS Nano* **2014**, *8*, 483–494.
[65] P. Gangadaran, X. J. Li, S. K. Kalimuthu, O. J. Min, C. M. Hong, R. L. Rajendran, H. W. Lee, L. Zhu, S. H. Baek, S. Y. Jeong, S. W. Lee, J. Lee, B. C. Ahn, *Sci. Rep.* **2018**, *8*, 13509.
[66] S. F. Mirshojaei, A. Ahmadi, E. Morales-Avila, M. Ortiz-Reynoso, H. Reyes-Perez, *J. Drug Targeting* **2016**, *24*, 91–101.
[67] C. M. Dundas, D. Demonte, S. Park, *Appl. Microbiol. Biotechnol.* **2013**, *97*, 9343–9353.
[68] A. K. Shukla, U. Kumar, *J. Med. Phys.* **2006**, *31*, 13–21.
[69] M. L. James, S. S. Gambhir, *Physiol. Rev.* **2012**, *92*, 897–965.
[70] Z. Varga, I. Gyurkó, K. Pálóczi, E. I. Buzás, I. Horváth, N. Hegedűs, D. Máthé, K. Szigeti, *Cancer Biother. Radiopharm.* **2016**, *31*, 168–173.
[71] S. Molavipordanjani, S. Khodashenas, S. M. Abedi, M. F. Moghadam, A. Mardanshahi, S. J. Hosseinimehr, *Eur. J. Pharm. Sci.* **2020**, *148*, 105312.
[72] M. I. González, P. Martín-Duque, M. Desco, B. Salinas, *Nanomaterials* **2020**, *10*, 1062.
[73] T. Smyth, M. Kullberg, N. Malik, P. Smith-Jones, M. W. Graner, T. J. Anchordoquy, *J. Controlled Release* **2015**, *199*, 145–155.
[74] F. N. Faruqu, J. T. Wang, L. Xu, L. McNickle, E. M. Chong, A. Walters, M. Gurney, A. Clayton, L. A. Smyth, R. Hider, J. Sosabowski, K. T. Al-Jamal, *Theranostics* **2019**, *9*, 1666–1682.
[75] S. Maji, A. Matsuda, I. K. Yan, M. Parasramka, T. Patel, *Am. J. Physiol. Gastrointest. Liver Physiol.* **2017**, *312*, G194–g200.
[76] X. Zhang, X. Yuan, H. Shi, L. Wu, H. Qian, W. Xu, *J. Hematol. Oncol.* **2015**, *8*, 83.
[77] C. H. Lu, Y. A. Chen, C. C. Ke, S. J. Chiu, C. C. Chen, Y. J. Hsieh, B. H. Yang, R. S. Liu, *Mol. Imaging Biol.* **2021**, *23*, 361–371.
[78] P. Gangadaran, C. M. Hong, B. C. Ahn, *BioMed Res. Int.* **2017**, *2017*, 9158319.
[79] M. Morishita, Y. Takahashi, M. Nishikawa, K. Sano, K. Kato, T. Yamashita, T. Imai, H. Saji, Y. Takakura, *J. Pharm. Sci.* **2015**, *104*, 705–713.
[80] S. Khairnar, N. More, C. Mounika, G. Kapusetti, *J. Med. Imaging Radiat. Sci.* **2019**, *50*, 575–589.
[81] L. Hu, S. A. Wickline, J. L. Hood, *Magn. Reson. Med.* **2015**, *74*, 266–271.
[82] A. Busato, R. Bonafede, P. Bontempi, I. Scambi, L. Schiaffino, D. Benati, M. Malatesta, A. Sbarbati, P. Marzola, R. Mariotti, *Int. J. Nanomed.* **2016**, *11*, 2481–2490.
[83] R. J. C. Bose, S. Uday Kumar, Y. Zeng, R. Afjei, E. Robinson, K. Lau, A. Bermudez, F. Habte, S. J. Pitteri, R. Sinclair, J. K. Willmann, T. F. Massoud, S. S. Gambhir, R. Paulmurugan, *ACS Nano* **2018**, *12*, 10817–10832.
[84] B. H. Kim, N. Lee, H. Kim, K. An, Y. I. Park, Y. Choi, K. Shin, Y. Lee, S. G. Kwon, H. B. Na, J. G. Park, T. Y. Ahn, Y. W. Kim, W. K. Moon, S. H. Choi, T. Hyeon, *J. Am. Chem. Soc.* **2011**, *133*, 12624–12631.
[85] Z. Shen, T. Chen, X. Ma, W. Ren, Z. Zhou, G. Zhu, A. Zhang, Y. Liu, J. Song, Z. Li, H. Ruan, W. Fan, L. Lin, J. Munasinghe, X. Chen, A. Wu, *ACS Nano* **2017**, *11*, 10992–11004.
[86] S. Rayamajhi, R. Marasini, T. D. T. Nguyen, B. L. Plattner, D. Biller, S. Aryal, *Biomater. Sci.* **2020**, *8*, 2887–2904.
[87] S. Aime, P. Caravan, *J. Magn. Reson. Imaging.* **2009**, *30*, 1259–1267.
[88] R. Chen, D. Ling, L. Zhao, S. Wang, Y. Liu, R. Bai, S. Baik, Y. Zhao, C. Chen, T. Hyeon, *ACS Nano* **2015**, *9*, 12425–12435.
[89] H. Wu, H. Xing, M. C. Wu, F. Shen, Y. Chen, T. Yang, *Theranostics* **2021**, *11*, 64–78.

Manuscript received: May 30, 2022
Revised manuscript received: August 1, 2022